Central depression in nuclear density and its consequences for the shell structure of superheavy nuclei

A. V. Afanasjev[1,2] and S. Frauendorf[1,3]
[1]*Department of Physics, University of Notre Dame, Notre Dame, Indiana 46556, USA*
[2]*Laboratory of Radiation Physics, Institute of Solid State Physics, University of Latvia, LV 2169 Salaspils, Miera str. 31, Latvia, and*
[3]*IKH, Research Center Rossendorf, Dresden, Germany*
(Received 5 October 2004; published 18 February 2005)

The influence of the central depression in the density distribution of spherical superheavy nuclei on the shell structure is studied within the relativistic mean-field theory. A large depression leads to the shell gaps at the proton $Z = 120$ and neutron $N = 172$ numbers, whereas a flatter density distribution favors $N = 184$ and leads to the appearance of a $Z = 126$ shell gap and to the decrease of the size of the $Z = 120$ shell gap. The correlations between the magic shell gaps and the magnitude of the central depression are discussed for relativistic and nonrelativistic mean field theories.

DOI: 10.1103/PhysRevC.71.024308 PACS number(s): 21.10.Ft, 21.10.Gv, 21.60.Jz, 27.90.+b

I. INTRODUCTION

The question of the possible existence of shell-stabilized superheavy nuclei and the precise location of the magic spherical superheavy nuclei has been in the focus of the nuclear physics community for more than three decades [1]. Unfortunately, the various theoretical models do not agree with respect to the magic shell gaps in superheavy nuclei. The proton numbers $Z = 114$, 120, and 126 and the neutron numbers $N = 172$ and 184 are predicted by different models and parametrizations [2]. All these models reproduce the known magic numbers in lighter systems. The predicted magic numbers are of decisive importance for the experimental search of superheavy nuclei. In such a situation it is necessary to understand what makes the predictions of the models so different in the region of superheavy nuclei. One of the reasons is the appearance of a central depression in the nuclear density [3,4], which is studied in this article.

The first predictions of superheavy nuclei were based on the shell correction method, which assumes a single-particle potential with a flat bottom. Nowadays, these calculations predict $Z = 114$ and $N = 184$. The microscopic self-consistent models start either from an effective nucleon-nucleon interaction (models based on the Skyrme and Gogny forces) or the exchange of mesons by nucleons [relativistic mean field (RMF) theory]. Although based on more fundamental principles, these models do not agree among each other in predicting the magic shell gaps of superheavy nuclei. In part, this is related to the fact that the reliability of different parametrizations of these models is verified only by comparing theoretical and experimental binding energies and their derivatives [separation energies, the $\delta_{2n,2p}(Z, N)$ quantities] and deformation properties [5]. These observables are not very sensitive to the energies of the single-particle states. For example, it was shown in Ref. [5] that the NLSH and NL-RA1 parametrizations of the RMF theory provide a reasonable description of these quantities in the deformed actinide region despite the fact that the single-particle energies are poorly reproduced. Accurate single-particle energies are crucial for predicting the shell gaps in superheavy nuclei. However, the accuracy of the description of the single-particle states in the deformed region of the heaviest actinides has been tested only for a few parametrizations of the RMF theory [5] and of the Skyrme SLy4 functional [6]. The shell correction approach is based on phenomenological potentials that best reproduce the single-particle levels of the actinides. However, the assumption of a flat-bottom radial profile is a severe source of error when extrapolating to the spherical superheavy nuclei.

Self-consistent microscopic calculations find a central depression in the nuclear density distribution [3,4], which generates a wine-bottle shaped nucleonic potential. Its magic numbers differ from the ones of the phenomenological flat-bottom potentials. The present manuscript studies the influence of this depression on the shell structure of spherical superheavy nuclei. As a theoretical tool we use the RMF theory for spherical nuclei without pairing [7] and the relativistic Hartree-Bogoliubov (RHB) theory [8,9].

II. DISCUSSION

Figure 1 compares the single-particle spectrum of a wine-bottle potential (g-s) with the one of a flat-bottom potential (exc-s). The details of the potentials are discussed later. The differences are easy to understand. The high-j orbitals are localized mostly near the surface, whereas the low-j orbitals have a more central localization (see, for example, Fig. 6.2 in Ref. [10]). As compared to a flat-bottom potential, the high-j orbitals are more and the low-j orbitals are less bound in an attractive wine-bottle potential. In the following it is useful to distinguish between the groups of low-j and high-j single-particle states. Filling up a low-j group with nucleons increases the density near the center, whereas filling a high-j group increases the density near the surface. As demonstrated, the occupation of these groups determines the radial profile of the neutron and proton densities and potentials.

We start with ^{208}Pb. The RMF theory provides a good description of the experimental charge density distribution of this nucleus [11,12]. With increasing neutron and proton numbers the corresponding densities are modified in the way

 ©2005 The American Physical Society

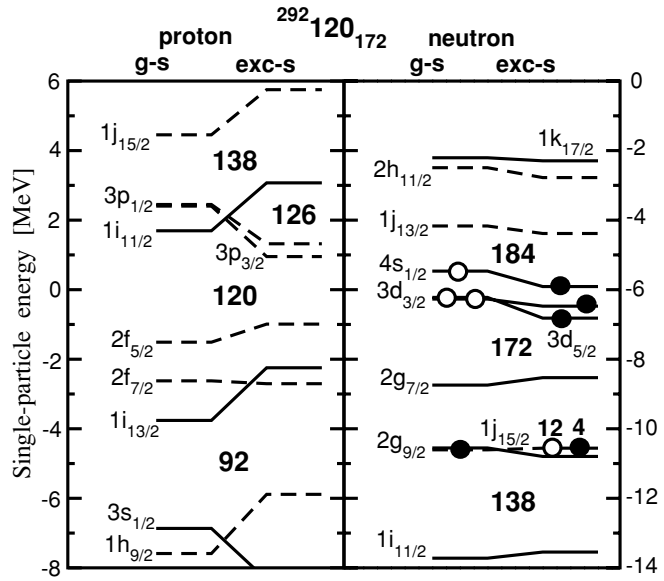

FIG. 1. Single-particle spectra of the ground state (indicated as g-s) and the excited (indicated as exc-s) configurations in the $^{292}120_{172}$ system obtained in the RMF calculations with the NL3 force. Solid and dashed lines are used for positive and negative parity, respectively. Solid and open circles indicate the occupied and empty orbitals, respectively. In the ground state, all subshells below $Z = 120$ and $N = 184$ are fully occupied. For the g-s configuration, the spin-orbit partners $3p_{1/2}, 3p_{3/2}$ and $3d_{3/2}, 3d_{5/2}$ show up at very close energy. In the excited configuration, only 12 particles are excited from the subshell $\nu 1j_{15/2}$: 4 particles still reside in this subshell. The spherical shell gaps of interest are indicated.

shown in Fig. 2. Between $Z = 82$ and $Z = 106$ the protons fill the high-j group $\pi 1i_{13/2}, \pi 1h_{9/2}$, between $Z = 106$ and $Z = 120$ they fill the medium-j group $\pi 2f_{7/2}, \pi 2f_{5/2}$, and between $Z = 120$ and $Z = 126$ they fill the low-j group $\pi 3p_{1/2}, \pi 3p_{3/2}$. The variation of the proton density is seen most clearly in the $N = 172$ isotones. The filling of the high-j group $\pi 1i_{13/2}, \pi 1h_{9/2}$ increases the density at the surface (compare $Z = 82$ and $Z = 106$ in Fig. 2). The filling of medium-j group $\pi 2f_{7/2}, \pi 2f_{5/2}$ increases the density between central and surface areas (see $Z = 120$). Finally, the filling of the low-j group $\pi 3p_{1/2}, \pi 3p_{3/2}$ increases the density in the central region of nucleus (see $Z = 126$).

The analogous polarization effects caused by the groups of low-j and high-j subshells in the neutron subsystem are illustrated in Fig. 2. The variation of the neutron density generated by filling these groups is seen most clearly in the $Z = 106$ isotopes. Filling the high-j group $\nu 1i_{11/2}, \nu 1j_{15/2}, \nu 2g_{9/2}$ increases the density near the surface. Filling the low-j group $\nu 3d_{5/2}, \nu 3d_{3/2}, \nu 4s_{1/2}$ increases the central density, and filling the high-j group $\nu 1j_{13/2}, \nu 2h_{11/2}, \nu 1k_{17/2}$ adds matter to the surface region. Analyzing the published results, we found that the grouping into high/medium/low-j subshells shown in Fig. 2 appears in all models/parametrizations (cf. Fig. 1 in the present manuscript and Figs. 4, 9, 13, and 15 in Ref. [3]).

As seen in Fig. 2, the combined occupation of the high-j neutron subshells $2g_{9/2}, 1j_{15/2}, 1i_{11/2}$ [and medium-j $2g_{7/2}$], and proton $1h_{9/2}$ and $1i_{13/2}$ [and medium-j $2f_{7/2}$] subshells leads to a central depression in the nuclear density between $Z = 106$ and $Z = 120$ and $N = 164$ and $N = 172$, which is especially pronounced in the $Z = 120$, $N = 172$ system. As seen from the density variations in Fig. 2, the proton subsystem plays a larger role in the creation of the central depression. This result differs from the results of the Skyrme calculations with the SkI3 parametrization [3], the authors of which claim that the central depression is mainly due to the occupation of the neutron subshells. The appearance of the central depression is a consequence of the different density distributions of the single-particle states: high-j orbits are located near the surface and low-j orbits near the center. This generic feature is dictated by the nodal structure of the wave functions in a leptodermic

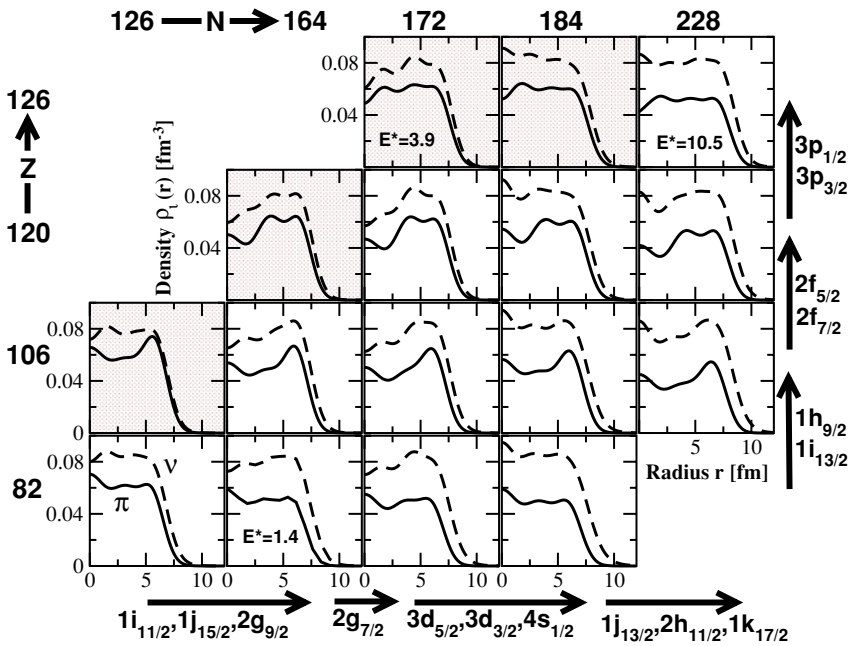

FIG. 2. The evolution of proton and neutron densities with the changes of proton and neutron numbers. Arrows indicate the group of single-particle subshells which become occupied with the change of the nucleon number. The figure is based on the results of spherical RMF calculations without pairing, employing the NL3 parametrization. The shaded background is used for nuclei located beyond the proton-drip line. If the indicated configuration is not lowest in energy, its excitation energy (in MeV) is given by E^*.

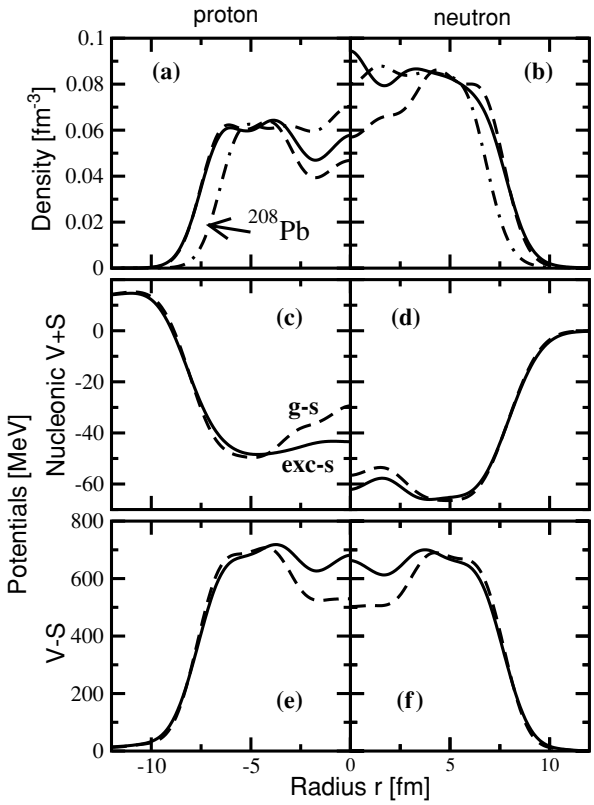

FIG. 3. Density distributions (upper row), nucleonic ($V + S$, middle row) and $V - S$ (bottom row) potentials in the ground (g-s) and excited (exc-s) configurations of $^{292}120_{172}$. S and V are the attractive scalar and repulsive vector potentials, respectively. The left column shows the proton system and the right the neutron system. The proton and neutron density distributions of ^{208}Pb are shown in upper panels for comparison.

potential. Hence, the high-j proton and neutron orbitals will modify the radial profile in a comparable way. However, the high-j proton orbitals should be more efficient, because the Coulomb interaction pushes them to larger radii. This is in contrast to the conclusions of Ref. [4] where it was stated that the reduction in the central density is the consequence of the large repulsive Coulomb energy.

Let us discuss the interplay among the geometry of the single-particle orbitals, the appearance of the central depression in the density, and the shell structure in more detail. One possibility to generate a flatter density distribution in the central part of nucleus is by exciting particles from high-j subshells to low-j subshells. Figure 1 shows an example of such an excitation in the $^{292}120_{172}$ system. Here 12 neutrons are excited from the $1j_{15/2}$ subshell into $3d_{5/2}$, $3d_{3/2}$, and $4s_{1/2}$ subshells. In this excited (called exc-s) configuration the neutron density distribution in the central part of nucleus is much flatter than in the ground state (called g-s) configuration, and its profile is very similar to the one in ^{208}Pb [Fig. 3(b)]. The changes in neutron density are fed back to the proton density, because the isovector interaction tries to keep them alike. As a consequence, the proton density distribution becomes also flatter [Fig. 3(a)] but the density fluctuations due to shell effects remain visible. Both the nucleonic potential $V + S$ [Figs. 3(c) and 3(d)] and the potential ($V - S$) [Figs. 3(e) and 3(f)], which in first approximation is related to the spin-orbit potential via $V_{\rm ls}(\mathbf{r}) = \frac{m}{m^*(\mathbf{r})}(V(\mathbf{r}) - S(\mathbf{r}))$ [14], reflect the density change: they becomes flatter in the central part of nucleus. This effect is especially pronounced in the proton nucleonic potential: the "wine-bottle" radial shape is replaced by a "flat-bottom" one. Another consequence of this excitation is an increase of the surface diffuseness both in the densities and in the potentials.

The various RMF forces are characterized by different compression moduli K_∞ (NL-Z [173 MeV], NL3 [272 MeV], and NLSH [355 MeV]). As expected, the magnitude of the central depression in the densities and potentials increases with the decrease of the compression modulus. However, the changes in the energies of single-particle states, densities, and potentials induced by our probing particle-hole excitation do not depend sensitively on the compressibility.

As a result of the flattening of the nucleonic potential the energies of the single-particle states are changed as described above (see Fig. 1). The shifts are larger in the proton subsystem because the proton potential is more flattened than the neutron one. The $Z = 126$ proton gap emerges and the size of the $Z = 120$ gap decreases. To a lesser extent, the $N = 172$ neutron gap decreases and the $N = 184$ gap increases. The flattening of the ($V - S$) potential increases the splitting of the spin-orbit pairs $[\pi 3p_{1/2}, \pi 3p_{3/2}]$, $[\nu 3d_{3/2}, \nu 3d_{5/2}]$, and $[\pi 2f_{5/2}, \pi 2f_{7/2}]$. The large spin-orbit splitting of the last pair of orbitals generates the $Z = 114$ shell gap predicted by a number of flat-bottom potentials. The present results clearly show that a flatter density distribution leads to a larger splitting between these orbitals.

We have studied further excitations that induce a flatter density distribution. In all cases we found the above-mentioned dependence of the size of the $Z = 120$, 126 and $N = 172$, 184 shell gaps on the magnitude of the central depression. Our results are consistent with the HFB studies with the Gogny D1S force, which employed an external potential to induce the central depression [4]: large $N = 184$ and $Z = 126$ shell gaps were found for the values of the external potential that generate a flat density distribution and large $Z = 120$ and $N = 172$ shell gaps for the values that generate a central depression (see Fig. 2 in Ref. [4]). However, Ref. [4] does not discuss how the central depression and corresponding shells gaps depend on particular choice of the external potential. On the contrary, our study of a considerable number of particle-hole excitations, which in the language of Ref. [4] would correspond to different choices of external potential, clearly indicate that above-mentioned features are general.

Because of the isovector force, which tries to keep the neutron and proton density profiles alike, there is a mutual enhancement of the $Z = 120$ and $N = 172$ gaps, both being favored by the wine-bottle potential, and of the $Z = 126$ and $N = 184$ gaps, both favored by the flat bottom potential. For the same reason the gaps are smaller for the combination $Z = 126$ and $N = 172$, and the $Z = 120$ gap does not develop for $N = 184$. This behavior is not expected to depend much on the density functional chosen. Indeed, a number of Skyrme calculations (SkI3, SkI4, SkI1, SLy6), which show a large $Z = 120$ gap in the $^{292}120_{172}$ system, do not show the double shell closure at $Z = 120$, $N = 184$ [15]. These generic features are

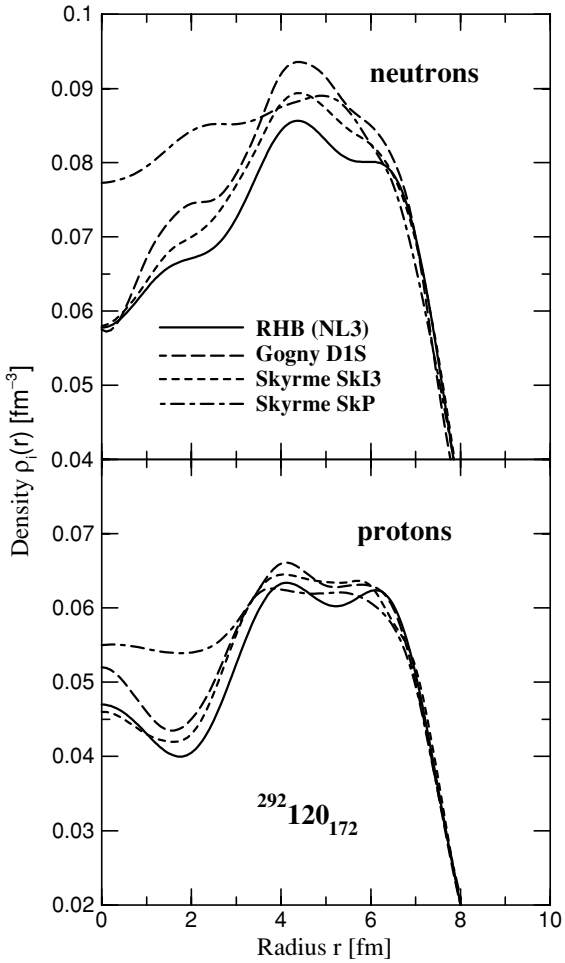

FIG. 4. Neutron and proton densities of the $^{292}120_{172}$ nucleus obtained in different models/parametrizations. The densities obtained with Skyrme and Gogny forces are taken from Refs. [3,13].

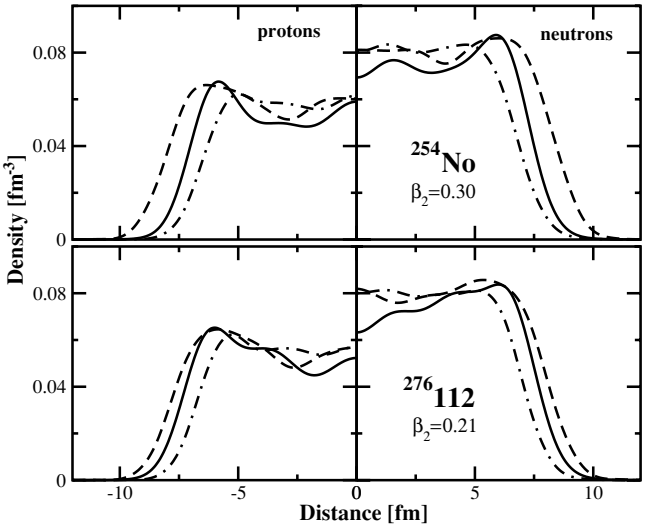

FIG. 5. Proton and neutron densities in deformed ground state (shown by dashed and dot-dashed lines) and excited spherical state (shown by solid lines) of ^{254}No and $^{276}112_{164}$ nuclei. They are shown as a function of radius (spherical shape) and as a function of distance along [most elongated profile] and perpendicular [least elongated profile] the symmetry axis. These results were obtained in the RHB theory [8] with approximate particle number projection by means of the Lipkin-Nogami method and with the NL3 set and the strength of the Gogny D1S force from Ref. [5]. Equilibrium deformations of deformed states are indicated.

also seen in the calculations with Gogny the D1S force (Fig. 2 in Ref. [13]), with the SkI1 (Fig. 2 in Ref. [15]), and SkI3, SkI4, SkP (Figs. 6, 7, and 8 in Ref. [3]) Skyrme forces, and with the RMF NL3 and NL-Z2 forces (Fig. 2 in Ref. [16]).

Let us consider the $^{292}120_{172}$ system, which is a doubly magic superheavy nucleus in RMF theory. Both the relativistic and the nonrelativistic (Gogny D1S, Skyrme parametrizations with low isoscalar effective mass m^*/m such as SkI3, SLy6 [3]) models show a pronounced central depression (see Fig. 4). These density functionals are characterized by similar values of m^*/m (Gogny D1S [$m^*/m = 0.67$], Skyrme SkI3 [$m^*/m = 0.57$], and SLy6 [$m^*/m = 0.69$] [3]. These values should be compared with the RMF Lorentz effective mass of the nucleon at the Fermi surface $m^*(k_F)/m \approx 0.66$ [3], because the effective mass is momentum-dependent in the RMF theory [17]. The central depression is much smaller in the Skyrme calculations with SkP (Fig. 4) and SkM* forces (Ref. [3]) which have high values of the isoscalar effective mass $m^*/m = 1$ and 0.789, respectively. The development of a more pronounced central depression for the density functionals with low effective mass may be understood as follows. In the surface region, the ratio m^*/m changes from low value (<1) in the interior to one in the exterior. Classically, nucleons with given kinetic energy are more likely to be found in regions with high effective mass than in the regions with low one because they travel with lower speed. This is reflected by the Thomas-Fermi expression for the nucleonic density $\rho \propto [2m^*(\epsilon_F - V)]^{3/2}$. The increase of the effective mass in the surface region favors the transfer of mass from the center there, which makes the above-discussed polarization mechanism of the high-j orbitals more effective for functionals with low effective mass. Based on this argument we suggest that a flatter radial profile is a generic feature of the density functionals with an effective mass close to 1. It would be interesting to investigate if the Skyrme functionals of this type systematically give flatter density distributions than the ones with a low effective mass.

All experimentally known nuclei with $Z \geqslant 100$ are expected to be deformed [1,18]. The deformation leads to a more even distribution of the single-particle states emerging from the high-j and low-j spherical subshells (see, for example, the Nilsson diagrams in Figs. 3 and 4 in Ref. [19]) than for spherical shape. Thus, the density profile of a deformed nucleus is flatter than of a spherical one (see Fig. 5), stronger resembling the density profile of phenomenological potentials. The RHB calculations also show that the density profiles of deformed nuclei change less drastically with particle number than that of spherical nuclei (see Figs. 2 and 5). In addition, the single-particle energies of the deformed nuclei in heavy actinide region have been carefully fitted in the phenomenological potentials. The combination of these factors explains the success of the shell correction method [20,21].

However, this method neglects the self-consistent rearrangement of single-particle levels caused by the appearance of a central depression in spherical superheavy nuclei. Thus, the predictions of the magic numbers for superheavy nuclei within the shell correction method should be considered with caution.

We have deliberately excluded from our study the forces NLSH and NL-RA1 [RMF] and SkI4 [Skyrme], which give a $Z = 114$ shell gap in self-consistent calculations. This is because they provide a poor description of either the energies of single-particle states in deformed actinide $A \sim 250$ nuclei [5,22] or of the spin-orbit splitting [3]. The energy splitting between deformed states emerging from the $2f_{7/2}$ and $2f_{5/2}$ subshells is well described by the RMF NL1 and NL3 [5] and Skyrme SLy4 [6] forces, which give a small $Z = 114$ shell gap. In our opinion, these results make the predicted shell gaps at $Z = 120$, 126 and $N = 172$, 184 most likely. As discussed above, their appearance and combination depends on the magnitude of the central depression. The RMF theory gives a pronounced double shell closure at $Z = 120$, $N = 172$. The nonrelativistic theories (Gogny [13], Skyrme [15,16]) give a large shell gap at $N = 184$ and less pronounced gaps at $Z = 120$ and 126, the size of which strongly depends on neutron number. For example, the Skyrme forces with high effective mass (SkM*, SkP) tend to predict a double shell closure at $Z = 126$, $N = 184$, whereas those with low effective mass (SkI1, SkI3, SkI4, SLy6) show a large gap at $Z = 120$ for $N = 172$, which becomes smaller or disappears when approaching $N = 184$.

In RMF theory, the $N = 172$ gap lies between the subshells $\nu 3d_{5/2}$ and $\nu 2g_{7/2}$, which form a pseudospin doublet [16]. The analysis of their deformed counterparts in the $A \sim 250$ region shows that the experimental energy distance between the pseudospin partners $\nu 1/2[620]$ and $\nu 3/2[622]$ is well reproduced, which supports the predicted existence of a gap at $N = 172$ (see Fig. 28 in Ref. [5]). However, taking into account the typical uncertainty of the description of the single-particle states in best-tested RMF parametrizations, one cannot exclude a large gap at $N = 184$ [5]. For this to take place, the energy of $\nu 4s_{1/2}$ state has to be overestimated by approximately 1 MeV.

III. CONCLUSIONS

In summary, the influence of the filling of the spherical subshells on the radial density profile and shell structure of superheavy nuclei has been studied. The occupation of high-j subshells decreases the density in the central part of the nucleus, the occupation of low-j subshells increases it. The polarization due to high-j orbitals generates a central depression of the density for nuclei with $Z \approx 120$ and/or $N \approx 172$. It is particularly pronounced for the combination $Z = 120$, $N = 172$, because both the proton and the neutron subsystems induce a central depression. Contrary to Refs. [3,4], our results for the first time clearly show the importance of the polarization effects in both subsystems for the creation of central depression. This large central depression produces large shell gaps at $Z = 120$ and $N = 172$. The occupation of low-j orbitals by means of either multi-particle-hole excitations or of the increase of Z, N beyond $Z = 120$, $N = 172$ removes the central depression and reduces these shell gaps. The shell gaps at $Z = 126$ and $N = 184$ are favored by a flat density distribution in the central part of nucleus. The magnitude of central density depression correlates also with the effective mass of nucleons: low effective mass favors a large central depression. The similarities and differences between nonrelativistic and relativistic mean-field models in predicting the magic shell gaps in spherical superheavy nuclei were discussed.

ACKNOWLEDGMENTS

The work was supported by DoE Grant DE-F05-96ER-40983.

[1] S. Hofmann and G. Münzenberg, Rev. Mod. Phys. **72**, 733 (2000).
[2] P.-G. Reinhard, M. Bender, and J. A. Maruhn, Comments Mod. Phys. **2**, A177 (2002).
[3] M. Bender, K. Rutz, P.-G. Reinhard, J. A. Maruhn, and W. Greiner, Phys. Rev. **60**, 034304 (1999).
[4] J. Decharge, J.-F. Berger, K. Dietrich, and M. S. Weiss, Phys. Lett. **B451**, 275 (1999).
[5] A. V. Afanasjev, T. L. Khoo, S. Frauendorf, G. A. Lalazissis, and I. Ahmad, Phys. Rev. C **67**, 024309 (2003).
[6] M. Bender, P. Bonche, T. Duguet, and P.-H. Heenen, Nucl. Phys. **A723**, 354 (2003).
[7] P. Ring, Prog. Part. Nucl. Phys. **37**, 193 (1996).
[8] A. V. Afanasjev, P. Ring, and J. König, Nucl. Phys. **A676**, 196 (2000).
[9] D. Vretenar, A. V. Afanasjev, G. Lalazissis, and P. Ring, Phys. Rep. (to be published).
[10] S. G. Nilsson and I. Ragnarsson, *Shapes and Shells in Nuclear Structure* (Cambridge University Press, Cambridge, 1995).
[11] Y. K. Gambhir, P. Ring, and A. Thimet, Ann. Phys. (NY) **198**, 132 (1990).
[12] P.-G. Reinhard, M. Rufa, J. Maruhn, W. Greiner, and J. Friedrich, Z. Phys. A **323**, 13 (1986).
[13] J.-F. Berger, L. Bitaud, J. Decharge, M. Girod, and K. Dietrich, Nucl. Phys. **A685**, 1c (2001).
[14] W. Koepf and P. Ring, Z. Phys. A **339**, 81 (1991).
[15] K. Rutz, M. Bender, T. Bürvenich, T. Schilling, P.-G. Reinhard, J. A. Maruhn, and W. Greiner, Phys. Rev. C **56**, 238 (1997).
[16] A. T. Kruppa, M. Bender, W. Nazarewicz, P.-G. Reinhard, T. Vertse, and S. Ćwiok, Phys. Rev. C **61**, 034313 (2000).
[17] M. Jaminon and C. Mahaux, Phys. Rev. C **40**, 354 (1989).
[18] Yu. Ts. Oganessian, Nucl. Phys. **A685**, 17c (2001).
[19] R. R. Chasman, I. Ahmad, A. M. Friedman, and J. R. Erskine, Rev. Mod. Phys. **49**, 833 (1977).
[20] P. Möller and J. R. Nix, J. Phys. G **20**, 1681 (1994).
[21] Z. Patyk and A. Sobiczewski, Nucl. Phys. **A533**, 132 (1991).
[22] M. Bender, Phys. Rev. C **67**, 019801 (2003).